Pergamon

Int. J. Multiphase Flow Vol. 22, No. 4, pp. 703–712, 1996

PII: S0301-9322(96)00010-9
0301-9322/96 $15.00 + 0.00

SOME CHARACTERISTICS OF AIR–WATER TWO-PHASE FLOW IN SMALL DIAMETER VERTICAL TUBES

K. MISHIMA and T. HIBIKI

Research Reactor Institute, Kyoto University, Kumatori-cho, Sennan-gun, Osaka 590-04, Japan

(Received 10 April 1995; in revised form 30 January 1996)

Abstract—Flow regime, void fraction, rise velocity of slug bubbles and frictional pressure loss were measured for air–water flows in capillary tubes with inner diameters in the range from 1 to 4 mm. Although some flow regimes peculiar to capillary tubes were observed in addition to commonly observed ones, overall trends of the boundaries between flow regimes were predicted well by Mishima–Ishii's model. The void fraction was correlated well by the drift flux model with a new equation for the distribution parameter as a function of inner diameter. The rise velocity of the slug bubbles was also correlated well by the drift flux equation. The frictional pressure loss was reproduced well by Chisholm's equation with a new equation for Chisholm's parameter C as a function of inner diameter. Copyright © 1996 Elsevier Science Ltd.

Key Words: gas–liquid flow, small diameter tube, capillary tube, flow measurement, flow regime, void fraction, pressure loss, neutron radiography

1. INTRODUCTION

Characteristics of gas–liquid two-phase flow in a small diameter tube have become important in relation to the cooling of a diverter of a fusion reactor and high power electronic devices. Since the effect of surface tension may be remarkable in a capillary tube, it is anticipated that the characteristics of gas–liquid two-phase flow differ from those in a round tube with a larger inner diameter, which, consequently, may affect the boiling heat transfer. For instance, it was reported that a buoyancy-driven bubble in a stagnant water could not rise in a capillary tube with a diameter below 5 mm (Gibson 1913; Zukoski 1966; Tung *et al.* 1976). In the same way, it is expected that such characteristics of two-phase flow as the flow regime, void fraction, rise velocity of slug bubbles and the pressure loss, differ from those in a larger diameter tube.

Although much work has been performed on gas–liquid two-phase flows in usual diameter tubes (JSME 1989; Ueda 1981), only a limited number of papers are available for capillary tubes (Sugawara *et al.* 1967; Barnea *et al.* 1983; Biswas & Greenfield 1985; Hijikata *et al.* 1985; Fukano *et al.* 1990, 1993; Kariyasaki *et al.* 1991, 1992; Ungar & Corwell 1992; Ide *et al.* 1993; Barajas & Panton 1993) with inner diameters in the order of millimeters. Among those, Fukano *et al.* (Fukano *et al.* 1992, 1993) performed extensive work on the characteristics of two-phase flow in capillary tubes, including the flow regimes, rise velocity of slug bubbles, void fraction, liquid film thickness and the pressure loss.

However it appears to be necessary to accumulate more data on flow characteristics to develop new equations to reproduce the effect of tube diameter quantitatively.

In view of this, the flow regime, void fraction, rise velocity of slug bubbles and the frictional pressure loss have been studied for two-phase flow in capillary tubes with inner diameters ranging from 1 to 4 mm.

2. EXPERIMENTAL

2.1. Apparatus

Four test sections, fabricated with round tubes made of Pyrex glass, were used in the experiment except in the measurement of void fraction. Their dimensions were shown in table 1. In the case of void fraction measurement, test sections were fabricated with round tubes made of aluminium alloy because of neutron penetration. Their dimensions were also shown in table 1. The test loop

Table 1. Dimensions of the test section

Diameter (mm)	Tube material	Entrance calming sect. (mm)	Pressure measuring sect. (mm)	Exit sect. (mm)
1.05	Glass	220	210	220
2.05	Glass	320	310	320
3.12	Glass	420	510	420
4.08	Glass	500	1000	500
1.09	Aluminum	140	440	140
2.10	Aluminum	140	440	140
3.08	Aluminum	140	440	140
3.90	Aluminum	500	1000	500

was the same as used in the previous experiment for rectangular ducts (Mishima *et al.* 1993). Working fluids were air and demineralized water. The water was circulated in the loop by a centrifugal pump. The flow rate of the water was measured by a float-type flow meter installed at just upstream of the inlet valve to the test section. The flow meter was calibrated at each temperature by comparing with the direct flow measurement by a measuring cylinder. The air was supplied by a compressor and was introduced into the test section along the center line of the tube through an injection nozzle installed at the entrance of the test section. The outer diameter of the injection nozzle was 0.5 mm. After flowing through the test section, the air was finally released into the atmosphere. The flow rate of the air was measured also by a float-type flow meter. The calibration curve was supplied by the fabricator. The air pressure was measured by a Bourdon-tube pressure gauge at the inlet of the flow meter and at just upstream of the outlet valve. The temperatures of air and water were measured using chromel-alumel thermocouples at the outlet of the flow meter and in a separator, respectively. The experiment was performed at the room temperature and near the atmospheric pressure.

2.2. *Measurement*

2.2.1. Flow regimes. Fluid behavior of two-phase flow was observed with a high-speed video camera, Kodak Ektapro-1000, at a speed of 1000 frames/s. Two-phase flow regimes were taken at the center of the pressure measuring section as shown in table 1. The images were then reproduced in slow motion for detailed observation.

2.2.2. Void fraction. The void fraction was measured with use of neutron radiography and image processing techniques (Mishima *et al.* 1992; Hibiki *et al.* 1993). A neutron beam, which penetrated horizontally across a vertical upward air-water flow in an aluminum test section, was attenuated in proportion to the thickness of the water layer along its path. Therefore, the neutron beam projected the image of two-phase flow which was changed into an optical image by a converter and detected with a high-sensitivity TV camera. Thus the image could be observed at real time. The average void fraction was measured from the brightness of the video images.

The experiment was performed by using the thermal neutron radiography facility No. 2 installed at the JRR-3M of the Japan Atomic Energy Research Institute. The combination of a scintillator (LiF + ZnS(Ag)), Kasei Opt., a silicon intensifier target tube, Hamamatsu C1000-12, and a lens, Canon V6X18R, was employed as an imaging system (Matsubayashi & Tsuruno 1994). The details of this method have been described in the previous paper (Hibiki *et al.* 1993). By this method, no systematic error was observed, and the time-averaged void fraction could be measured within the relative error of $\pm 5\%$ (i.e. relative mean deviation from the average of measured values) except at very small void fraction.

2.2.3. Rise velocity of slug bubbles. The rise velocity of a slug bubble was measured from consecutive images of the bubble reproduced in slow motion by the high-speed video, and was calculated based on the time for the bubble to rise a given distance at the center of the pressure measuring section. The measuring distance varied with the tube diameter, but was so short that the pressure loss across the measuring distance was estimated to be 1.5 and 5% of the total pressure loss for 1 mm i.d. and 4 mm i.d. tubes, respectively. Therefore, the effect of expansion on the slug bubble velocity was small. Then the average rise velocity was calculated by averaging the velocities of six slug bubbles at a given experimental condition. The velocities of small and cap bubbles were not taken into account in this measurement. The overall error in the measurement of the average rise velocity was estimated to be within $\pm 10\%$.

2.2.4. Frictional pressure loss. The overall pressure loss in the pressure measuring section as shown in table 1 was measured with three differential pressure transducers. The frictional pressure loss was calculated by neglecting the pressure loss due to the acceleration of the fluids and subtracting the pressure loss due to gravity from the overall pressure loss. The measurement errors for pressure losses of single-phase and two-phase flows were estimated to be within 1 and 5%, respectively.

In a capillary tube, the accuracy of the inner diameter may affect significantly the reliability of the measured value. The inner diameter was determined by using the analytical solution of the friction factor for laminar flow as follows.

The friction factor for single phase laminar flow in a round tube is given by the following well-known equation for Hagen–Poiseuille flow:

$$\lambda = \frac{64}{\mathrm{Re}} \qquad [1]$$

where Re: Reynolds number, λ: friction factor. Assuming a guess value for inner diameter, the friction factor and the Reynolds number were calculated from the experimental data, and the guess value was changed iteratively until the relationship between the friction factor and the Reynolds number was correlated by [1], then the inner diameter was determined. The error of the inner diameter so obtained was estimated to be within $\pm 2\%$.

3. RESULTS AND DISCUSSION

3.1. Flow regime

The sketch of typical flow regimes observed in a capillary tube is shown in figure 1. In this figure the asterisks denote flow regimes which are special for a capillary tube, whereas the other sketches show flow regimes observed in both larger diameter and capillary tubes.

The special flow regimes for a capillary tube have following characteristics. In bubbly flows, bubbles tend to concentrate along the tube axis. Smaller bubbles form a spiral train, while larger bubbles with the diameter just as large as the tube inner diameter line up right next to each other to form intermittent bubble trains, without coalescing. In slug flows, slug bubbles are relatively long and have a beautiful spherical nose. Bridges of very thin liquid film are observed in a long slug bubble. In liquid slugs, restlessly oscillating small bubbles are observed. In churn flows, long

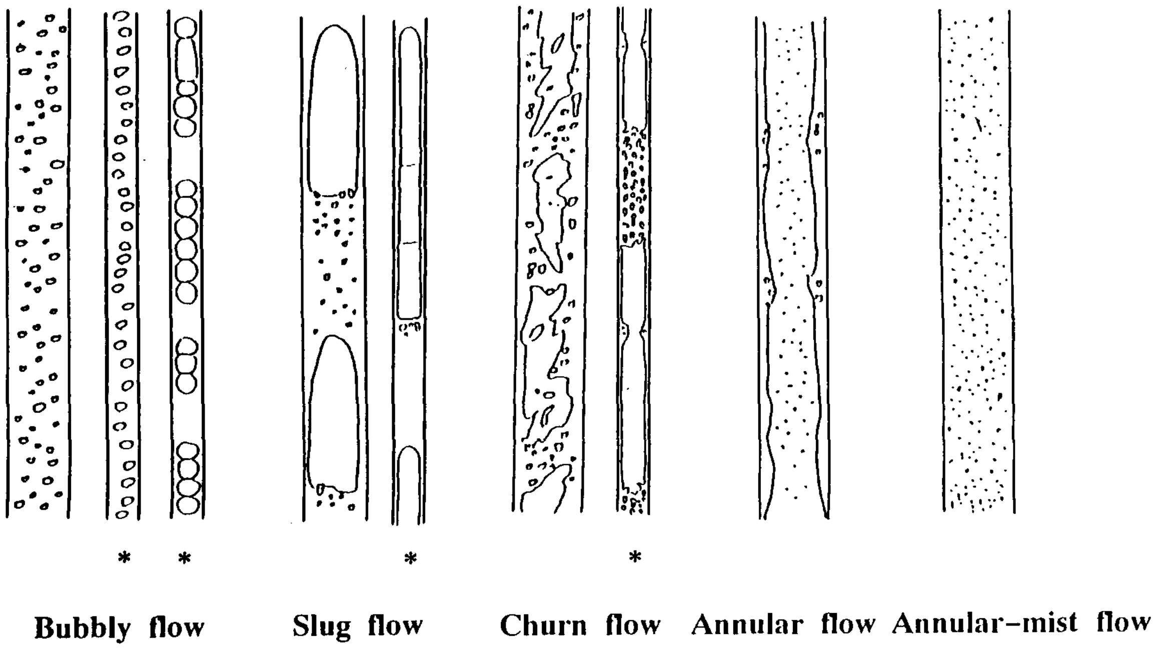

Figure 1. Observed flow regimes.

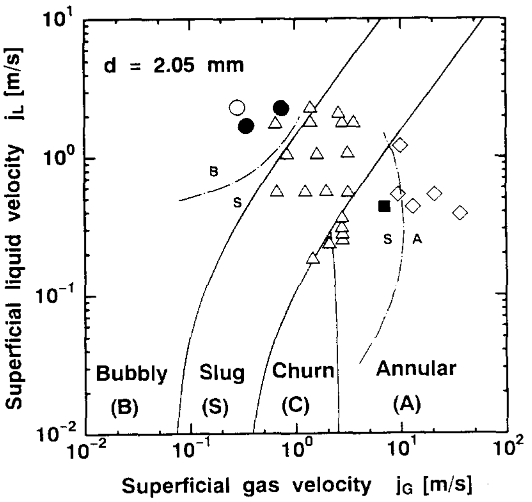

Figure 2. Flow regime map for $d = 2.05$ mm.

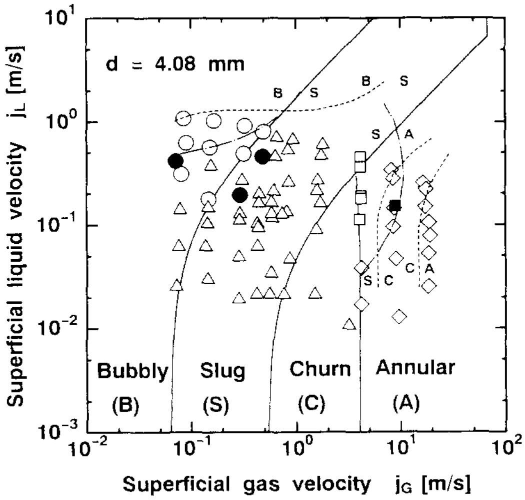

Figure 3. Flow regime map for $d = 4.08$ mm.

slug bubbles are deformed and do not have a spherical nose any more. A number of tiny bubbles are observed moving rapidly in liquid slugs.

The flow regime maps for inner diameters $d = 2.05$ and 4.08 mm are shown in figures 2 and 3, respectively. Similar results were obtained for $d = 1.05$ and 3.12 mm. In these figures, the vertical and horizontal axes mean the superficial velocities of liquid and gas, j_L and j_G, respectively. The open symbols denote clearly-identified flow regimes, and the solid symbols denote those not-clearly identified, i.e. flow regimes in transition regions. The solid lines represent the prediction by Mishima–Ishii's model (Mishima & Ishii 1984), while the dashed ones delineate the flow regime boundaries reported by Barnea *et al.* (1983) for a round tube with 4 mm diameter. Finally the chain lines represent the transition boundaries reported by Kariyasaki *et al.* (1992) who observed flow regimes in vertical round tubes with diameters in the range from 1.0 to 4.9 mm. These figures show that all the transition boundaries from three sources agree fairly well qualitatively with each other, if one takes into account the differences in the definition of flow regimes. As Mishima–Ishii's prediction reproduce the boundaries very well, it was clarified that their model could be applicable to a capillary tube as well.

3.2. *Void fraction*

Measured void fractions were correlated by the drift flux (D–F) model, i.e. the gas velocity v_G was calculated by j_G/ϵ where ϵ denotes the measured void fraction, and was plotted as a function of the mixture volumetric flux $j\ (=j_G + j_L)$, where the superficial velocities were measured at *in situ* conditions. According to the D–F model, the relationship between the gas velocity and the mixture volumetric flux can be expressed by the following equation:

$$v_G = j_G/\epsilon = C_0 j + V_{Gj} \qquad [2]$$

where C_0: distribution parameter and V_{Gj}: drift velocity.

In a round tube, the distribution parameter and the drift velocity are given by the following equations (Ishii 1977):

bubbly flow:

$$C_0 = 1.2 - 0.2\sqrt{\rho_G/\rho_L} \qquad [3]$$

$$V_{Gj} = (1 - \epsilon)^{3/2}\sqrt{2}(\sigma g \Delta\rho/\rho_L^2)^{1/4} \qquad [4]$$

slug flow:

$$C_0 = 1.2 - 0.2\sqrt{\rho_G/\rho_L} \qquad [5]$$

$$V_{Gj} = 0.35\sqrt{\Delta\rho g d/\rho_L} \qquad [6]$$

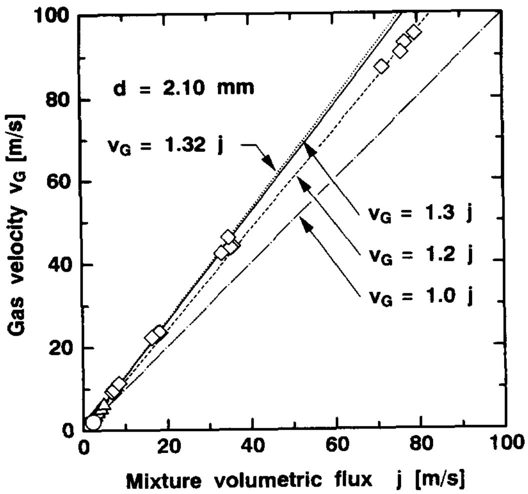

Figure 4. D–F correlation of the void fraction for $d = 1.09$ mm.

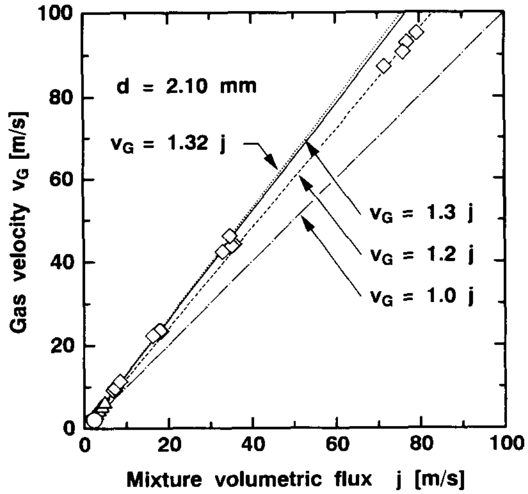

Figure 5. D–F correlation of the void fraction for $d = 2.10$ mm.

churn flow:

$$C_0 = 1.2 - 0.2\sqrt{\rho_G/\rho_L} \quad [7]$$

$$V_{Gj} = \sqrt{2}(\sigma g \Delta\rho/\rho_L^2)^{1/4} \quad [8]$$

annular flow:

$$C_0 = 1.0 \quad [9]$$

$$V_{Gj} = \frac{(1-\epsilon)\left[j + \sqrt{\dfrac{\Delta\rho g d(1-\epsilon)}{0.015\rho_L}}\right]}{\epsilon + 4\sqrt{\rho_G/\rho_L}} \quad [10]$$

where ρ_G: density of the gas, ρ_L: density of the liquid, σ: surface tension, g: the gravitational acceleration, $\Delta\rho$: differences between the liquid and gas densities.

The results are shown in figures 4 and 5 for $d = 1.09$ and 2.10 mm, respectively, where the same symbols as in figures 2 and 3 are used to denote the flow regime for each data point. Similar results were obtained for $d = 3.08$ and 3.90 mm, respectively. In these figures, the lines to express the correlation were drawn assuming the drift velocity of the bubbly and slug flows to be zero, since the rising velocity of bubbles in stagnant water becomes zero in a capillary tube (Gibson 1913). This trend was observed by the previous studies (Zukoski 1966; Tung & Parlange 1976; Kariyasaki *et al.* 1992), too. Therefore, the correlation for the present cases can be expressed as follows:

$$v_G = C_0 j. \quad [11]$$

The distribution parameters C_0 in bubbly and churn flows calculated from [3] and [7] are 1.19, while the present results determined by the least-squares method are $C_0 = 1.45$, 1.31, 1.33 and 1.21

Table 2. Database for correlation of the distribution parameter C_0

Data source	Diameter (mm)	Superficial velocity (m/s)		Reynolds number	
		Gas	Liquid	Gas	Liquid
Present work	1.09	2.20–18.6	0.453–0.907	177–1710	542–1080
	2.10	0.579–79.3	0.0884–1.67	86.8–12200	215–3990
	3.08	0.263–38.9	0.119–1.26	54.2–8350	415–4260
	3.90	0.0896–33.5	0.0116–0.860	24.9–9580	48.6–3720
Kariyasaki (1992)	1.0	0.079–6.57	0.1–2.0	4.76–396	125–2490
	2.4	0.113–11.4	0.03–2.0	16.3–1648	89.7–5978
	4.9	0.111–10.1	0.03–2.0	32.8–2981	183–12204

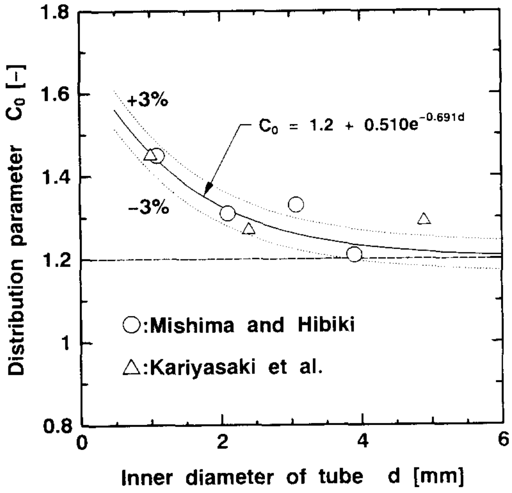

Figure 6. Distribution parameter C_0 as a function of d.

for $d = 1.09$, 2.10, 3.08 and 3.90 mm, respectively, where data for annular flow with $j > 30$ m/s are not included. The results are shown with open circles in figure 6. Open triangles represent data taken by Kariyasaki *et al.* (1992) who originally correlated the void fraction ϵ in terms of the gas volumetric flux ratio β $(=j_G/(j_G+j_L))$ instead of the D–F model. It is seen that the agreement between their data and ours is good, and the distribution parameter for bubbly and slug flows is a decreasing function of inner diameter and can be correlated by the following equation:

$$C_0 = 1.2 + 0.510\mathrm{e}^{-0.691d} \qquad [12]$$

where the unit of d should be in mm. The database for this equation is summarized in table 2. This equation reproduces all the data within the standard deviation of 2.5%. In figure 6, dotted lines denote the predictions including $\pm 3\%$ deviations.

It should be noted also that the data points for the mixture volumetric flux larger than about 10 m/s fell slightly below the correlation line. Those data were taken in the annular flow condition. Similar tendency was reported also in the previous study (Mishima *et al.* 1993) for rectangular ducts with a narrow gap, i.e. the distribution parameter increased when the gap is very narrow. These tendencies for small diameter tubes and narrow rectangular ducts may be attributed to the centralized void profile and the laminarization of the flow in such narrow channels.

Bendiksen (1985) discussed the dependency of the distribution parameter C_0 on the surface tension and the Reynolds number for a slug bubble rising in a forced flow in a vertical tube. They presented correlations for the distribution parameter both for laminar and turbulent flows. The equations were given as functions of the inverse Eotwos number and the Reynolds number. The tested values of the inverse Eotwos number were smaller than 0.1 whereas those in the present study were larger than 1. Therefore, Bendiksen's equations may not be applicable to the present experimental conditions. Nevertheless, their equations predict a larger slug bubble velocity for a laminar flow, which is consistent with the present result.

3.3. Rise velocity of slug bubbles

The average rise velocity of slug bubbles, u_B, was correlated in the same manner as the D–F correlation for void fraction. The results are shown in figures 7 and 8 for the inner diameters $d = 1.05$ and 4.08 mm, respectively. Similar results were obtained for $d = 2.05$ and 3.12 mm. Solid and dashed lines represent the predictions by the following equations:

$$u_B = C_B j \qquad [13]$$

where the values of the parameter C_B are indicated in the figures, respectively. It is seen that all the data points are in between the two lines, which means that the slope of the line is between 1.0 and 1.2, i.e. approximately $C_B = 1.1$, and that the slope does not depend much on the tube diameter. Fukano *et al.* (1990) reported that the slope increased from 1.09 to 1.21 when the tube diameter

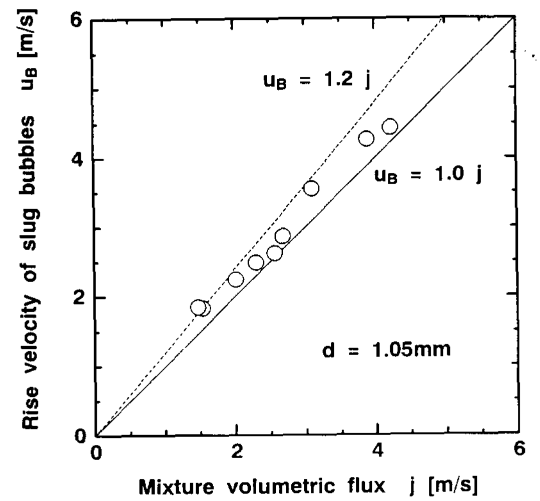

Figure 7. Rise velocity of slug bubbles for $d = 1.05$ mm.

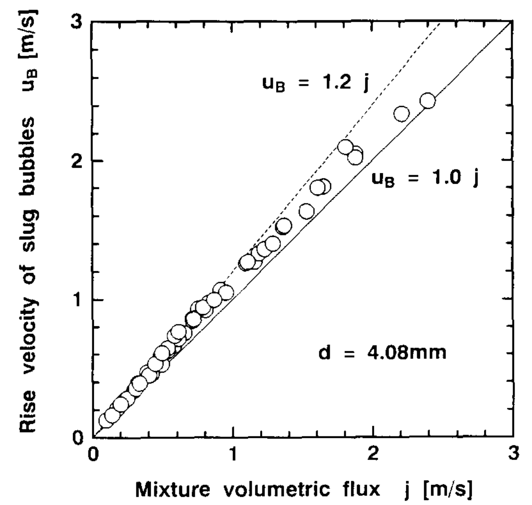

Figure 8. Rise velocity of slug bubbles for $d = 4.08$ mm.

decreased from 4.9 to 1 mm, but the difference between their results and ours appears to be within the measurement error.

It is also noted in figures 7 and 8 that the rise velocity tends to approach the line expressed by $u_G = 1.0j$ when the mixture volumetric flux increases. This result is apparently different from that shown in figures 4 and 5. The reason of this can be explained as follows. As mentioned before, the rise velocity of slug bubbles u_B was measured excluding small and cap bubbles, while the gas velocity v_G was measured including all the bubbles. In a small diameter tube, slug bubbles are rather long so that a slug bubbles section behaves like an annular flow in which the distribution parameter approaches to 1.0. On the other hand, small cap bubbles tend to concentrate along the centerline of the tube and drift faster than slug bubbles, which makes the distribution parameter for v_G larger. This may be the reason for the difference of the distribution parameters for u_B and v_G.

3.4. *Frictional pressure loss*

Concerning the frictional pressure loss for a single-phase turbulent flow, it is only mentioned here that the result indicated that the Blasius equation was also applicable to capillary tubes. Concerning the frictional pressure loss for two-phase flow, Lockhart–Martinelli's (L–M) method (Lockhart & Martinelli 1949) was used, i.e. the data were plotted in terms of the two-phase multiplier ϕ_L^2 and the Lockhart–Martinelli parameter X as defined by the following equations:

$$\phi_L^2 = \frac{\Delta P_T}{\Delta P_L} \qquad [14]$$

$$X^2 = \frac{\Delta P_L}{\Delta P_G} \qquad [15]$$

where ΔP_L, ΔP_G: frictional pressure losses when either the liquid or the gas component flowed in the tube as a single-phase flow, respectively. The results are shown in figures 9 and 10, for $d = 2.05$ and 3.12 mm, where the open circles denote the experimental data and the solid lines denote modified Chisholm's equation (Chisholm 1967):

$$\phi_L^2 = 1 + \frac{C}{X} + \frac{1}{X^2} \qquad [16]$$

where C: Chisholm's parameter. The value of original Chisholm's parameter was given depending upon whether the flow of each component is laminar or turbulent. For example, when both phases are turbulent, $C = 21$, but it is independent of the tube diameter. However, as seen in figures 9 and 10, the present value of Chisholm's parameter decreases with decreasing the tube diameter.

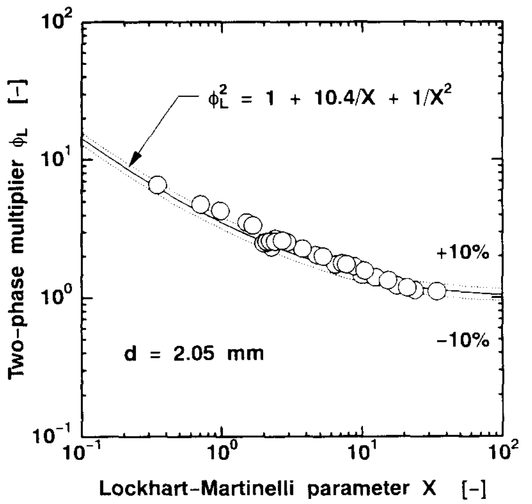

Figure 9. L–M correlation for $d = 2.05$ mm.

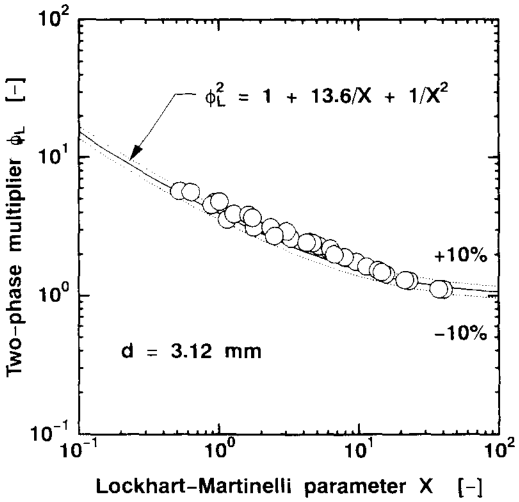

Figure 10. L–M correlation for $d = 3.12$ mm.

Thus, together with the results for $d = 1.05$ and 3.12 mm, modified Chisholm's parameter is given by:

$$C = 21(1 - e^{-0.333d}) \qquad [17]$$

where d: tube inner diameter [mm]. Similar result was obtained by Sugawara *et al.* (1967) for horizontal capillary tubes. In figure 11, [17] is compared with the present data together with the data taken by Sugawara *et al.* (1967) as well as those for ammonia–vapor flow in round tubes by Ungar & Corwell (1992). Thus it is shown that [16] with [17] is applicable to both vertical upward and horizontal flows in a capillary tube. Furthermore, in the previous study (Mishima *et al.* 1993) for narrow rectangular ducts, Chisholm's parameter C was expressed by a similar equation, where the hydraulic diameter $d_e = 2sw/(s + w)$ was used instead of tube diameter, where s and w were the gap and the width of the duct, respectively. Thus a new equation, which can be expressed as follows, was developed for vertical and horizontal round tubes as well as rectangular ducts.

$$C = 21(1 - e^{-0.319d_e}). \qquad [18]$$

The database for this equation is shown in table 3. The comparison of [18] with the data is shown in figure 12 which demonstrates a good agreement. Therefore, [18] could be used for vertical and horizontal round tubes as well as vertical and horizontal rectangular ducts. This equation predicted all the data in table 3 except those for ammonia–vapor flow within an error of $\pm 12\%$. For the

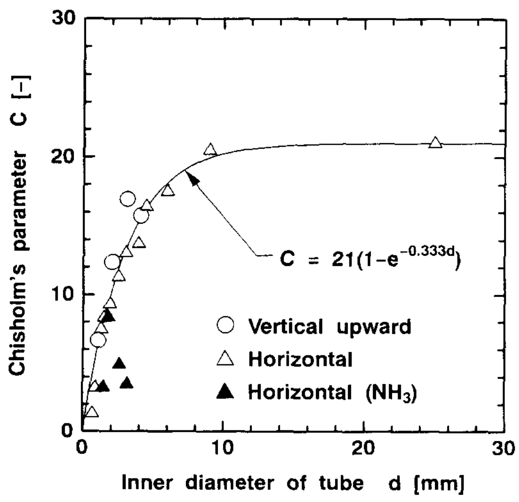

Figure 11. Parameter C as a function of tube diameter.

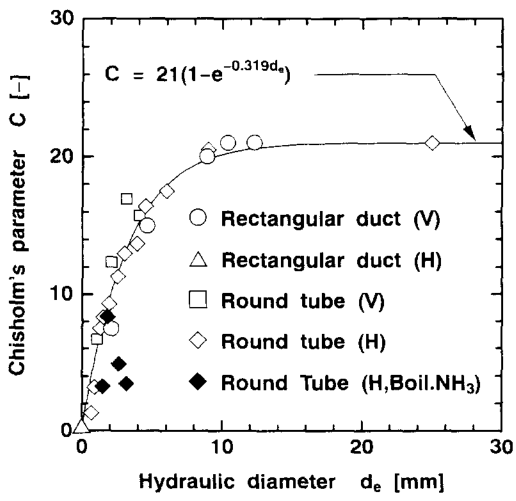

Figure 12. Parameter C for round tubes and rectangular ducts.

Table 3. Database for correlation of parameter C in Chisholm's equation

Data source	Geometry	Working fluids	Flow direction	Diameter or gap × width (mm)	Superficial gas velocity (m/s)	Superficial liquid velocity (m/s)
Present work	Round tube	Air–Water	Vertical upward	1.05	1.20–49.4	0.153–2.23
				2.05	0.354–37.4	0.185–2.33
				3.12	0.196–16.5	0.152–2.11
				4.08	0.0711–18.9	0.0714–1.06
Sugawara (1967)	Round tube	Air–Water	Horizontal	0.7–9.1	Not clear	Not clear
Ungar (1992)	Round tube	Ammonia–Vapor	Horizontal	1.46–3.15	Not clear	Not clear
Mishima (1993)	Rectangular duct	Air–Water	Vertical upward	1.07 × 40	0.1–50	0.5–5
				2.45 × 40	0.05–20	0.2–8
				5.00 × 40	0.02–7	0.08–1
Sadatomi (1982)	Rectangular duct	Air–Water	Vertical upward	(7–17) × 50	Not clear	Not clear
				7 × 20.6		
Moriyama (1992)	Rectangular duct	$R113\text{–}N_2$	Horizontal	0.007 × 30	0.1–0.6	0.002–0.015
				0.025 × 30	0.3–4	0.01–0.15
				0.052 × 30	0.1–7	0.005–0.43
				0.098 × 30	0.1–7	0.03–0.22

data for ammonia–vapor flow, the error becomes 25%. It should be noted here that the value of parameter C becomes zero when the hydraulic diameter is as small as 0.2 mm (Moriyama *et al.* 1992).

4. SUMMARY

Experimental study was performed for air–water two-phase flow in capillary tubes with the diameters in the range from 1 to 4 mm, and the following results were obtained for flow regime, void fraction, rising velocity of slug bubbles and frictional pressure loss:

(a) The bubble shape was largely affected by capillary force and the flow regimes peculiar to a capillary tube were observed. The boundaries between the flow regimes were reproduced well by Mishima–Ishii's model.
(b) The void fraction was correlated well by the drift flux model with zero drift velocity and a newly developed equation for the distribution parameter as a function of the tube diameter.
(c) The average rise velocity of slug bubbles was also correlated by the drift flux model with zero drift velocity and the approximate distribution parameter equal to 1.1.
(d) The two-phase frictional pressure loss was correlated well by Chisholm's correlation with newly developed equation for parameter C as a function of the tube diameter.

Acknowledgements—The authors wish to express their gratitude to Messrs A. Tsuruno and M. Matsubayashi of the Japan Atomic Energy Research Institute for their collaboration in performing the neutron radiography experiment. Part of this work was supported by the Grants-in-Aid for International Scientific Research, University-to-University Cooperative Research from the Ministry of Education, Science and Culture (No. 02045020) in 1990–1992.

REFERENCES

Barajas, A. M. & Panton, R. L. 1993 The effect of contact angle on two-phase flow in capillary tubes. *Int. J. Multiphase Flow* **19**, 337–346.

Barnea, D., Luninski, Y. & Taitel, Y. 1983 Flow pattern in horizontal and vertical two phase flow in small diameter pipes. *Can. J. Chem. Engng* **61**, 617–620.

Bendiksen, K. H. 1985 On the motion of long bubbles in vertical tubes. *Int. J. Multiphase Flow* **11**, 797–812.

Biswas, J. & Greenfield, P. F. 1985 Two-phase flow through vertical capillaries—existence of a stratified flow pattern. *Int. J. Multiphase Flow* **11**, 553–563.

Chisholm, D. 1967 A theoretical basis for the Lockhart–Martinelli correlation for two-phase flow. *Int. J. Heat Mass Transfer* **10,** 1767–1778.

Fukano, T., Kariyasaki, A. & Kagawa, M. 1990 Flow patterns and pressure drop in isothermal gas–liquid concurrent flow in a horizontal capillary tube. *Trans. JSME (Ser. B)* **56,** 2318–2326, in Japanese.

Fukano, T. & Kariyasaki, A. 1993 Characteristics of gas–liquid two-phase flow in a capillary tube. *Nucl. Eng. Design* **141,** 59–68.

Gibson, A. H. 1913 On the motion of long air-bubbles in a vertical tube. *Phil. Mag.* **26,** 952–965.

Hibiki, T., Mishima, K., Yoneda, K., Fujine, S., Kanda, K., Nishihara, H., Tsuruno, A. & Matsubayashi, M. 1993 Application of neutron radiography to visualization and void fraction measurement of air–water two-phase flow in a small diameter tube. *J. Nucl. Sci. Technol.* **30,** 516–523.

Hijikata, K., Mori, Y., Nagasaki, T. & Nohata, K. 1985 A study on high speed two-phase flow through a capillary tube. *Trans. JSME (Ser. B)* **51,** 1033–1041, in Japanese.

Ide, H., Matsumura, H. & Kado, H. 1993 Velocity of liquid lumps in vertical upward gas–liquid two-phase flow in capillary tubes (effect of tube diameter in annular flow). *Trans. JSME (Ser. B)* **59,** 795–801.

Ishii, M. 1977 One-dimensional drift–flux model and constitutive equations for relative motion between phases in various two-phase flow regimes. ANL Report ANL-77-47.

JSME (Ed.) 1989 *Handbook of Gas–Liquid Two-phase Flow Technology.* Corona Publ., Tokyo, Japan, in Japanese.

Kariyasaki, A., Fukano, T., Ousaka, A. & Kagawa, M. 1991 Characteristics of time-varying void fraction in isothermal air–water cocurrent flow in a horizontal capillary tube. *Trans. JSME (Ser. B)* **57,** 4036–4043, in Japanese.

Kariyasaki, A., Fukano, T., Ousaka, A. & Kagawa, M. 1992 Isothermal air–water two-phase up- and downward flows in a vertical capillary tube (1st report, Flow pattern and void fraction). *Trans. JSME (Ser. B)* **58,** 2684–2690, in Japanese.

Lockhart, R. W. & Martinelli, R. C. 1949 Proposed correlation of data for isothermal two-phase, two-component flow in pipes. *Chem. Eng. Prog.* **5,** 39–48.

Matsubayashi, M. & Tsuruno, A. 1994 JRR-3 neutron radiography facility. In *Neutron Radiography* (4) (Edited by J. P. Barton). Gordon & Breach, New York, pp. 415–422.

Mishima, K., Fujine, S., Yoneda, K., Yonebayashi, K., Kanda, K. & Nishihara, H. 1992 A study of air-water flow in a narrow rectangular duct using an image processing technique. In *Dynamics of Two-phase Flows* (Edited by O. C. Jones & I. Michiyoshi). CRC Press, New York, pp. 141–160.

Mishima, K., Hibiki, T. & Nishihara, H. 1993 Some characteristics of gas–liquid flow in narrow rectangular ducts. *Int. J. Multiphase Flow* **19,** 115–124.

Mishima, K. & Ishii, M. 1984 Flow regime transition criteria for upward two-phase flow in vertical tubes. *Int. J. Heat Mass Transfer* **27,** 723–737.

Moriyama, K., Inoue, A. & Ohira, H. 1992 The thermohydraulic characteristics of two-phase flow in extremely narrow channels (the frictional pressure drop and void fraction of adiabatic two-component two-phase flow). *Trans. JSME (Ser. B)* **58,** 401–407.

Sadatomi, Y., Sato, T. & Saruwatari, S. 1982 Two-phase flow in vertical noncircular channels. *Int. J. Multiphase Flow* **8,** 641–655.

Sugawara, S., Katsuta, K., Ishihara, I. & Muto, T. 1967 Consideration on the pressure loss of two-phase flow in small-diameter tubes. In *Proc. 4th National Heat Transfer Symp. of Japan,* 169–172, in Japanese.

Tung, K. W. & Parlange, J. Y. 1976 Note on the motion of long bubbles in closed tubes—influence of surface tension. *Acta Mechanica* **24,** 313–317.

Ueda, T. 1981 *Gas–Liquid Two-phase Flow.* Yokendo Publ., Tokyo, Japan, in Japanese.

Ungar, E. K. & Corwell, J. D. 1992 Two-phase pressure drop of ammonia in small diameter horizontal tubes. AIAA 92-3891.

Zukoski, E. E. 1966 Influence of viscosity, surface tension, and inclination angle on motion of long bubbles in closed tubes. *J. Fluid Mech.* **25,** 821–837.